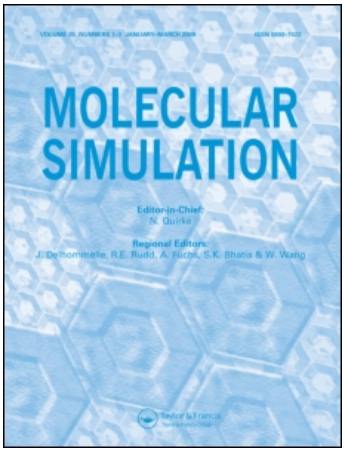

Molecular Simulation
Publication details, including instructions for authors and subscription information:
http://www.informaworld.com/smpp/title~content=t713644482

Underpotential deposition of hydrogen on Pt(111): a combined direct molecular dynamics/density functional theory study

Juan J. Mateo[a]; Donald A. Tryk[a]; Carlos R. Cabrera[a]; Yasuyuki Ishikawa[a]
[a] Department of Chemistry and the Chemical Physics Program, University of Puerto Rico, San Juan, PR, USA

To cite this Article Mateo, Juan J. , Tryk, Donald A. , Cabrera, Carlos R. and Ishikawa, Yasuyuki(2008) 'Underpotential deposition of hydrogen on Pt(111): a combined direct molecular dynamics/density functional theory study', Molecular Simulation, 34: 10, 1065 — 1072
To link to this Article: DOI: 10.1080/08927020802178591
URL: http://dx.doi.org/10.1080/08927020802178591

Molecular Simulation
Vol. 34, Nos. 10–15, September–December 2008, 1065–1072

Taylor & Francis
Taylor & Francis Group

Underpotential deposition of hydrogen on Pt(111): a combined direct molecular dynamics/density functional theory study

Juan J. Mateo, Donald A. Tryk, Carlos R. Cabrera and Yasuyuki Ishikawa*

Department of Chemistry and the Chemical Physics Program, University of Puerto Rico, San Juan, PR, USA

(*Received 31 January 2008; final version received 3 May 2008*)

A combined direct molecular dynamics/density functional theoretical study of the electro-oxidation of molecular hydrogen at the Pt(111)/water interface has been carried out to provide insights into the adsorbed underpotential deposition (UPD) states of hydrogen at submonolayer coverages of bridging hydrogen atoms $H_{ads(bridge)}$. As in our previous study, H_2 oxidation proceeds via the Heyrovsky process, forming a hydrated H^+ ion and an UPD hydrogen atom, which is strongly adsorbed and is lying nearly flat in a bridging position on the Pt(111) surface. At submonolayer coverage, the UPD $H_{ads(bridge)}$ atoms spontaneously self-assemble to form a hexagonal 2D honeycomb network on the Pt(111) surface, a signature that could be considered to be characteristic of UPD states of hydrogen.

Keywords: electro-oxidation; hydrogen; underpotential deposition of hydrogen; direct molecular dynamics

1. Introduction

The electrocatalytic behaviour of platinum in the cathodic hydrogen evolution reaction (HER) and anodic hydrogen oxidation reaction (HOR), particularly the influence of the various low-index crystal faces, has been intensively studied during the last several years, partly because of the technological potential of hydrogen-based fuel cells [1]. An archetypical process in electrocatalysis, the HOR on platinum, in spite of such study, remains to be fully elucidated in terms of the mechanistic details, including the extent of involvement of the various types of adsorbed hydrogen species, for example, the adsorbed underpotential deposition (UPD) states of hydrogen [1–29]. Because of the complexity of the redox reactions at the electrode/electrolyte interface, the atomistic details of the electrocatalysis remain a subject of much study [30–44].

An array of experimental techniques has been used to study the detailed mechanisms of the HER/HOR and the adsorbed UPD states of hydrogen [1–29,42,43]. Surface structural and surface spectroscopic techniques [6,14,21,27,28] have provided the most detailed look yet at the HOR/HER reactions on the atomic scale. Of particular interest has been the quest to correlate the reaction kinetics with the adsorption of reaction intermediates, with varying degrees of surface selectivity [19]. The detailed analysis of UPD hydrogen adsorption states on Pt(100) provided evidence for three states [4]. Less strongly bound states of H existing at potentials near that of the reversible hydrogen electrode (RHE) and in the so-called overpotential deposition (OPD) region, i.e. negative of 0.0 V versus RHE, have been thought to participate in the HER, as argued by Conway and Jerkiewicz [23]. The UPD coverage θ_H increases continuously from zero at $\sim +0.35$ V versus RHE to a limiting value as the potential approaches 0.0 V [8]. The H_{ads} intermediate that is involved in the kinetics, therefore, was considered to be a special type of adsorbed state, i.e. OPD H, which is adsorbed in addition to the UPD H, already covering the electrode and in particular, residing at sites different from those at which UPD H resides. These observations are fully consistent with our recent theoretical identification of $H_{ads(top)}$ as OPD H and $H_{ads(bridge)}$ as UPD H, which occupy different sites and possess quite different spectroscopic and energetic properties [44].

The kinetics of HER on well-ordered Pt single crystal electrodes has become rather well understood [12,13,16]. It has been concluded confidently that on all of the Pt single crystal surfaces, UPD H cannot be an intermediate in the HER. This conclusion is consistent with *in situ* surface vibrational spectroscopic results [6,43]. For example, *in situ* infrared (IR) spectroscopic results have shown the presence of a Pt—H stretching vibration on Pt(111) at potentials lower than 0.11 V versus RHE [6]. The frequency of this species is consistent with the on-top configuration. Kunimatsu et al. [43] have used surface-enhanced IR absorption spectroscopy and electrochemical kinetic analysis on polycrystalline Pt to establish that the H atom adsorbed at atop sites, $H_{ads(top)}$, is the reaction intermediate in HER, and the recombination of two $H_{ads(top)}$ atoms is the rate-determining step. Adzic and coworkers have carried out convincing kinetic analysis of the HOR on polycrystalline Pt and have concluded that there is a dual pathway, one

*Corresponding author. Email: yishikawa@uprrp.edu

ISSN 0892-7022 print/ISSN 1029-0435 online

DOI: 10.1080/08927020802178591
http://www.informaworld.com

involving homolytic cleavage ($H_2 \rightarrow 2H_{ads}$) and the other heterolytic cleavage ($H_2 \rightarrow H_{ads} + H^+ + e^-$) [42]. This is expected, since the mechanism has been shown to differ on the different crystal faces [16].

Ab initio correlated methods [30–33], density functional theory (DFT) [34,35] and first-principles molecular dynamics (MD; [36,40]) have been used increasingly to probe various types of reaction environments and to obtain atomic-level understanding. Recent examples include methanol oxidation [40] and oxygen reduction on Pt [39], water activation on Pd [34], and on alloy and sequentially deposited Pt/Ru surfaces [35,41]. Complete reaction pathways have been identified and trends in reactivity have been elucidated. In a previous study [44], we have conducted a first-principles direct MD study for the Pt(111)/acid electrolyte interface to conclude that the HOR proceeds via the Heyrovsky process and that the reaction products are the $H^+_{(aq)}$ and an inert bridging hydrogen, $H_{ads(bridge)}$, which we identify as the UPD hydrogen (H_{UPD}).

In the present study, the mechanistic details of the HOR on Pt(111) are examined in greater detail in the presence of $H_{ads(bridge)}$ preadsorbed on the metal surface at submonolayer coverages by use of first-principles direct MD simulation [39,40,44,45] and DFT methods. We have continued to address the adsorbed UPD states of hydrogen and their possible involvement in the electrocatalytic processes. The mechanisms for the formation of adsorbed UPD states at submonolayer coverage are still not well understood and thus, a detailed first-principles theoretical study is expected to complement previous experimental and theoretical studies. With this study, together with future work, we hope to approach an understanding of the relationship between the electrocatalytic behaviour of the anodic HOR and the adsorbed UPD/OPD states of hydrogen at low- and high-coverage states at the Pt(111)/water interface; the latter is a contributing factor in controlling the kinetics of the HOR in aqueous hydrogen–oxygen fuel cells [42].

2. Computational method and metal/water interface modelling

In this section, we outline the metal/water interface modelling and computational methods employed in this study. The geometric structure of the $Pt_{38}(111)$ model electrocatalyst, composed of two 19-atom layers, which was employed in several earlier studies, is displayed in Figure 1 [35,44,46]. The bulk Pt—Pt bond distance from experimental data (cell parameter $a = 3.92$ Å) was initially adopted for the model clusters. Relaxation was permitted only for those metal atoms (shown in light green in Figure 1) of the surface layer more directly involved in the reaction. The binding energies of hydrogen in four different adsorption sites on two- and three-layer clusters, and with and without water layers were presented previously [44]. Our results obtained with the two-layer cluster model agree well with experiment

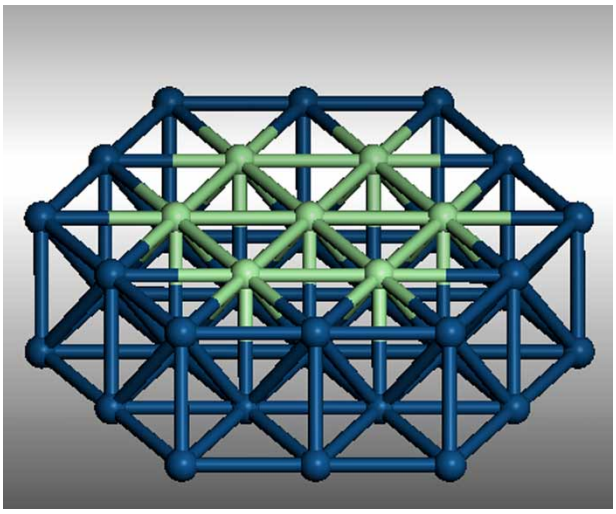

Figure 1. $Pt_{38}(111)$ cluster model structure used in the calculations. The metal atoms of the surface layer for which relaxation was permitted are shown in light green.

and previous DFT slab calculations for the gas–solid interface [47–49], in which hollow sites are favoured for H adsorption. The effect of the slab/cluster thickness is small, well within 1 kcal/mol.

Up to 22 water molecules were introduced to create a solvated environment [34,35,41]. This number leads to the density of water of 0.96 g/cm^3 in the solvent phase. All of the solvent water molecules and the surface layer Pt atoms were allowed to move freely during the structure optimisations. The solvation environment clearly favoured a heterolytic cleavage of the H—H bond where the separation of charges in the transition state (TS) and products was effectively stabilised by the ambient water molecules. In order to control the effective electrode potential, the Pt cluster was charged (q representing the charge in the system) by adding (or removing) a given number of electrons to (or from) the system, in a manner similar to that discussed by other investigators, including Wang and Balbuena [39], Hartnig and Spohr [40], and Filhol and Neurock [34]. As in our previous study [44], the electrode potential U_q was estimated from the ionisation energy $Ø_q$ relative to that of the standard hydrogen electrode $Ø_{SHE}$,

$$U_q = Ø_q - Ø_{SHE}.$$

The activation energy curves for the most important unitary steps in the HOR (Heyrovsky reaction) and HER (Volmer reaction) at different electrode potentials were presented in Figure 6 of [44].

The geometries of the cluster-adsorbate-water structures were optimised in DFT calculations using DMol^3 (Accelrys Inc., San Diego, CA, USA; [50]). The DNP basis sets [50] – numerical basis sets of double-zeta + polarisation quality – were used in the optimisations. Perdew–Burke–Ernzerhof (PBE; [51]) exchange

and correlation functionals were employed. An all-electron scalar relativistic algorithm was employed in conjunction with the density functionals in DMol^3 to obtain the correct energetics [35]. In a large metal cluster, a number of low-lying unoccupied orbitals exist very close energetically to the ground state (~0.1 eV). In our calculations, the fractional occupation number technique [50] was employed, where electrons are 'smeared' by an energy width of 0.1 eV over the orbitals around the Fermi energy. The resulting total energy may be viewed as an average over configurations lying energetically close to the ground state of the cluster.

Dynamics studies have been conducted with the technique of direct *ab initio* MD developed and implemented in our group [44,45]. Direct MD is a quasiclassical Born–Oppenheimer simulation in which quantum chemical electronic structure calculations are done at each time step to evaluate energy gradient in the classical evolution of the positions of the atomic nuclei. The potential surface is thus generated 'on the fly', rather than fit to an analytic form beforehand. The artistry necessary to construct an accurate surface is avoided, but generating the surface on the fly restricts reactive system dynamics from being examined in as much detail as they can be on a fitted surface. For systems more complex than tetratomic, however, the direct MD is the more practical approach and it has opened the door to accurate simulation of the dynamics of complex systems.

The solution of the classical equations of motion in Newtonian form

$$\frac{\mathrm{d}}{\mathrm{d}t}\left(m_i\dot{\mathbf{r}}_i\right) = -\nabla_{\mathbf{r}_i}E, \quad i = 1, \ldots, 3N,$$

determines the nuclear trajectories. Here, N is the number of nuclei in the system and m_i the mass of the i-th nucleus. The Verlet explicit central difference method is employed to integrate the equations of motion. Energies and gradients were evaluated by use of DMol^3. The Verlet algorithm with time steps of 0.5 fs was employed to integrate the classical equations of motion. To simulate the metal/water interface, up to 22 water molecules were introduced and were allowed to 'rain down' towards the Pt surface [39,40]. H_2 and solvent water molecules began each trajectory with vibrational, but no rotational energy at any given electrode potential. No zero-point vibrational energy was given for the Pt_{38} cluster. The initial temperature T of the system was calculated from the total kinetic energy, which was scaled to 300 K.

$$\sum_i m_i v_i^2/2 = (3N - 6)kT/2,$$

where v_i is the velocity of the i-th nucleus.

The solvent water molecules, hydrogen and all metal atoms were allowed to move freely during the direct MD simulation. The presence of the relatively large number of water molecules allowed the H^+ oxidation product to fluctuate between a variety of structures, such as $H_5O_2^+$ (Zundel ion) and $H_9O_4^+$ [52]. Initial H_2–metal surface separations of 2.5–3.5 Å were chosen. A total of four trajectories were started and all were reactive. More details of the computations can be found in our most recent study [44].

3. Results and discussion

3.1 Direct dynamics simulation of HOR

Direct *ab initio* MD calculations for the HOR were performed with submonolayer coverages of $H_{ads(bridge)}$ atoms on the Pt(111) surface in order to examine the adsorbed UPD states of hydrogen. Figures 2 and 3 illustrate

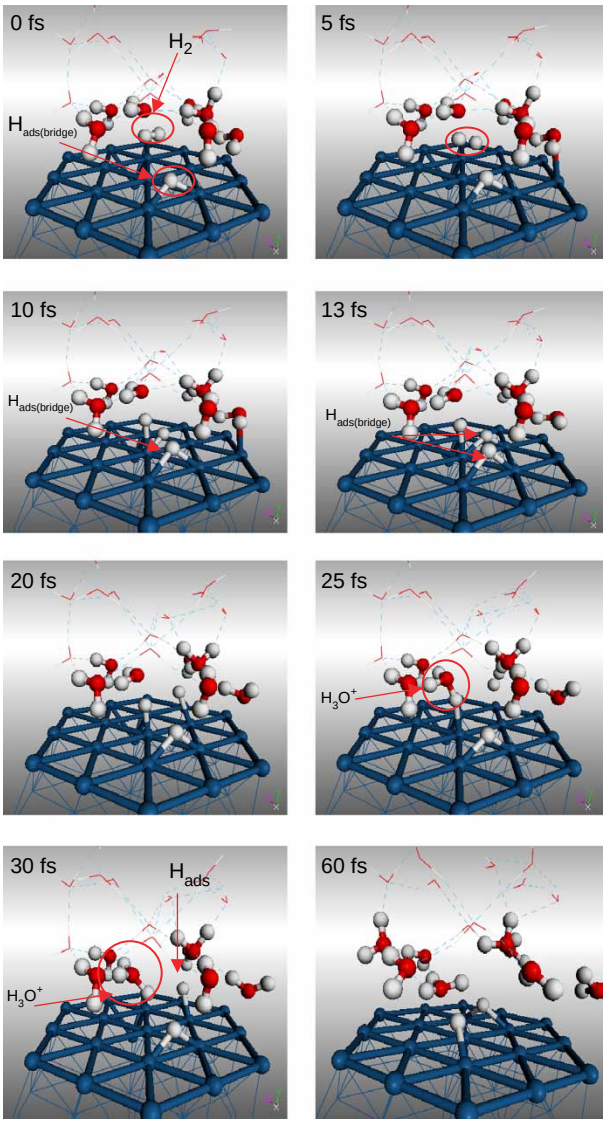

Figure 2. H_2 oxidation in the presence of one $H_{ads(bridge)}$: a sequence of atomic configurations in a sample MD trajectory at ~ + 0.3 V versus RHE.

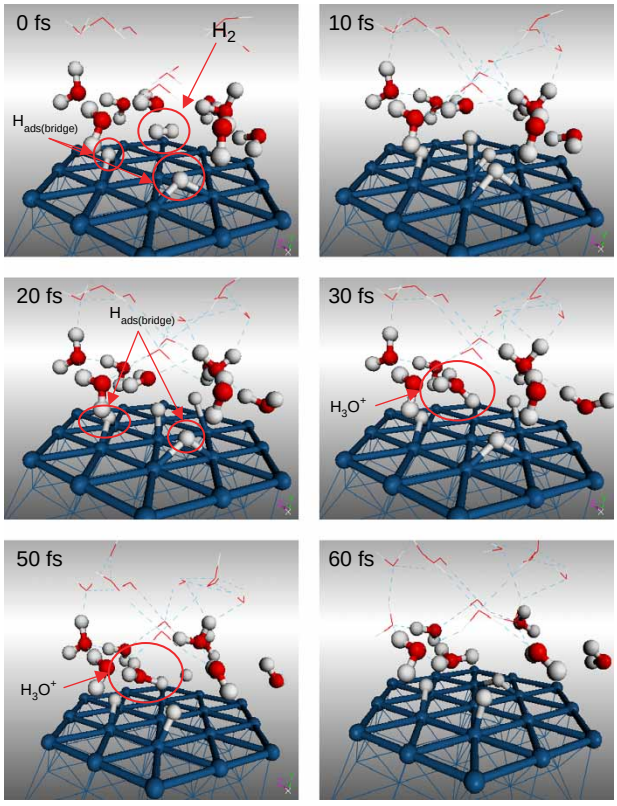

Figure 3. H_2 oxidation in the presence of two $H_{ads(bridge)}$: a sequence of atomic configurations in a sample MD trajectory at $\sim +0.3$ V versus RHE.

sequences of configurations in the H_2—Pt surface reaction in the presence of one and two $H_{ads(bridge)}$ atoms, respectively, at a relatively positive electrode potential (+0.3 V versus RHE). The trajectories exemplify all of the reactive surface processes in which the solvated H_2 molecule makes side-on and end-on approaches to the Pt(111) surface.

The reaction mechanism was simple, as observed in our earlier study [44]. At the beginning of the trajectory, an H_2 molecule was placed along the bottom layer of solvating water molecules and was drawn to the metal surface by H_2—Pt attraction (5 fs). Common to all trajectories was the approach of the hydrogen molecule to the nearest Pt on the surface and a subsequent rapid heterolytic dissociation, i.e. an oxidative adsorption, of the surface-bound H_2 via the Heyrovsky pathway to form a proton and a bridging hydrogen $H_{ads(bridge)}$ on the femtosecond time scale (at 10–20 fs), followed by rapid site-to-site shifts (>30 fs) of the bridging hydrogen atom just produced. While the surface-adsorbed hydrogen atoms already present are perturbed slightly (50 fs), they remain in bridge sites on the femtosecond time scale. The bridging hydrogen atom, although, it can readily migrate from site to site by breaking and then re-making a bond to Pt, lies nearly flat on the surface and interacts very little with the aqueous media, a primary reason for the stability of $H_{ads(bridge)}$ with respect

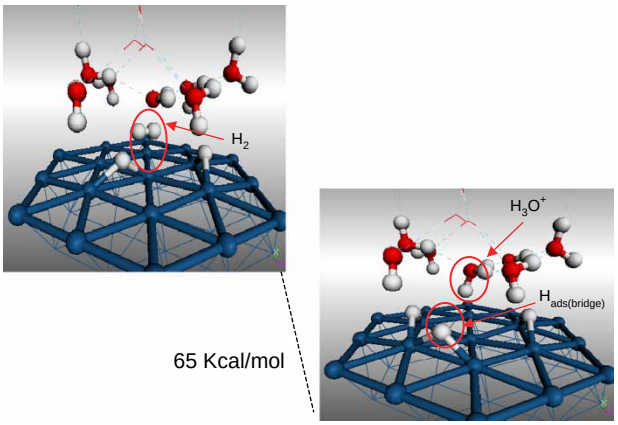

Figure 4. Diagram of relative energies of the reactant and product asymptotes on the $H_2/2H_{ads(bridge)}/Pt_{38}$/water potential energy surface at $\sim +0.3$ V versus RHE.

to oxidation. There was no sign of oxidation for any of the bridging hydrogen atoms at potentials up to $\sim +0.3$ V versus RHE, strongly indicating that these atoms ($H_{ads(bridge)}$) are part of what is collectively referred to as a submonolayer of H_{UPD}.

A diagram of relative DFT energies of reactant and product asymptotes on the $H_2/2H_{ads(bridge)}/Pt_{38}$/water potential energy surface at the potential of zero total charge ($\sim +0.2$ V versus RHE) is displayed in Figure 4. The surface oxidation reaction is exothermic by 65 kcal/mol and proceeds through a barrierless heterolytic H—H bond breaking step to form a $H_{ads(bridge)}$ and a solvated proton. The 65 kcal/mol of energy released upon exothermic formation of proton and bridging hydrogen goes into the product internal energy, imparting a series of rapid $H_{ads(bridge)}$ and proton migrations. The heterolytic reaction and the formation of hydrated proton and UPD hydrogen revealed in the MD trajectories is not inconsistent with the experimental study of Markovic et al. [16]; these authors concluded that for Pt(111) the heterolytic (Heyrovsky–Volmer) nor homolytic (Tafel–Volmer) mechanism could be uniquely established. In the present work, the $H_{ads(bridge)}$ atoms are stable even at potentials much more positive (0.2–0.3 V versus RHE) than the reversible potential and possess electronic and vibrational properties characteristic of H_{UPD} [44]. We are in the process of mapping the potential dependence of the adsorption in order to check for consistency with the Frumkin isotherm [16].

3.2 *UPD states of adsorbed hydrogen*

The stabilities of H adsorption on hollow, bridge, and on-top sites were studied at the Pt(111)/water interface, as reported earlier [44]. As mentioned earlier, for gas phase adsorption, a chemisorbed H occupies hollow sites with multi-fold coordination and is more strongly bound than those adsorbed atop Pt [53]. Because, the chemisorbed

H atoms are most stable at hollow sites at the Pt(111)/gas interface, all previous studies of the aqueous system have assumed the UPD hydrogen to occupy hollow sites at the metal/water interface as well. At the Pt(111)/water interface, however, we found that the chemisorbed hydrogen no longer occupies hollow sites as it is no longer a stable minimum [44]. All geometry optimisations attempting to locate the atom at the threefold hollow site at potentials <0.1 V versus RHE led to either on-top or bridging adsorption in the presence of the solvent. Comparison of the theoretical bond energy for $Pt—H_{ads(bridge)}$ with that for $Pt—H_{UPD}$ experimentally determined further substantiates our identification of bridging hydrogen as H_{UPD} (see below).

In a recent computational study, Skúlason et al. found that, for 7/6 monolayer (ML) coverage of hydrogen at the Pt(111)/water interface at potentials more negative than the reversible potential, 1 ML hydrogen adsorbs at a mixture of face-centered cubic (FCC, hollow) and bridging sites, with the additional fraction, 1/6 ML, at on-top sites [54]. The authors mention that on-top H atoms interact with the FCC H atoms, pushing the latter to bridging sites. Although, such an interaction no doubt could be present, in our results, it does not account for the fact that the bridging sites are more favoured even when the on-top H atoms are absent (see below). We propose that this difference is due to the inclusion of all electrons in the present calculations.

Zolfaghari et al. [17] and Markovic et al. [19] determined the $Pt(111)—H_{UPD}$ bond energy, corresponding to the dissociation energy $Pt—H_{UPD}/water \rightarrow Pt/water + H_{(vac)}$, in the UPD potential region (0.05–0.375 V versus RHE) to be 57–60 kcal/mol, obtained in alkali and acid solutions. The theoretical binding energy, 55.6 kcal/mol, which we computed near the reversible potential, is in good agreement with these experimental values [44].

DFT geometry optimisations were conducted to identify the structure of submonolayer coverage of three H_{UPD} atoms in the $+0.2$ to $+0.3$ V versus RHE potential range. Figure 5 displays a diagram of the relative energies of the $3H_{ads(bridge)}/Pt_{38}$/water potential energy surface at the potential of zero total charge ($\sim +0.2$ V versus RHE) before and after the structure optimisation of the three $H_{ads(bridge)}$ atoms. At the outset of the structure optimisation, the adsorption sites of the three $H_{ads(bridge)}$ atoms were randomly chosen (left panel in Figure 5). All geometry optimisations that began with a variety of surface structures of the three H_{UPD} invariably led to a unique self-assembled, boat-shaped configuration, shown in the right panel. The rearrangement of the three $H_{ads(bridge)}$ at this surface potential is exothermic by 10 kcal/mol and proceeds through a barrierless process. This arrangement of the three H_{UPD} atoms can be seen to be a precursor of the honeycomb formation that develops with higher coverage (see below). As with the isolated

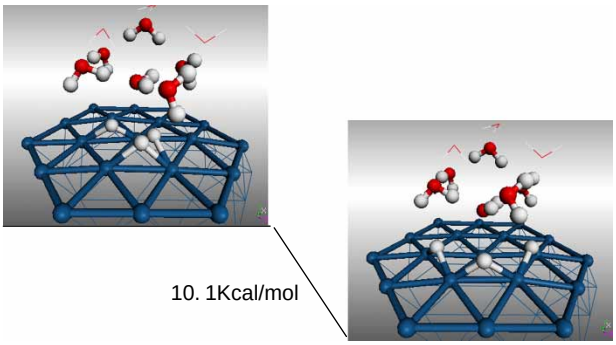

Figure 5. Diagram of relative energies of the $3H_{ads(bridge)}/Pt_{38}$/water system before and after self-assembly process at the potential of zero total charge ($\sim +0.2$ V versus RHE).

H_{UPD} atoms shown in Figure 2, these lie nearly flat on the metal surface and interact very little with ambient water molecules. Unlike $H_{ads(top)}$, which forms a strong hydrogen bond with ambient water [44] and is readily oxidised at potentials of $\sim +0.1$ V and above, there is no sign of hydrogen bonding between the H_{UPD} and any of the water molecules in the solution phase. Therefore, there is little change in the structure of the solution phase during the $H_{ads(bridge)}$ reorganisation process. The average distance between the bridging hydrogen and the oxygen atoms of the nearest water molecules is 3.3 Å, i.e. too large for hydrogen bonding.

Normal mode analysis clearly showed an absence of involvement of ambient water molecules in the $Pt—H_{ads(bridge)}$ stretch perpendicular to the surface [44]. In that study, the harmonic stretching frequency 1090 cm^{-1} was predicted for a single $H_{ads(bridge)}$ interacting with an adjacent $H_{ads(top)}$ at 0.0 V versus RHE. We have also found that a number of IR-active $Pt—H_{ads(bridge)}$ stretching frequencies appear in two ranges, 1000–1100 cm^{-1} and 1400–1500 cm^{-1} at submonolayer H_{UPD} coverage [55]. Nichols and Bewick were unable to detect the $Pt—H_{ads(bridge)}$ stretching, but pointed out that a frequency near 1050 cm^{-1} would be expected for hydrogen in a bridging site, based on the results of high-resolution electron energy loss spectroscopy [56]. In a recent study, Kunimatsu et al. [43] employed surface-enhanced IR absorption spectroscopy to identify a band at 1050 cm^{-1} that increased in intensity as the potential was lowered from $+0.12$ to -0.03 versus RHE at a polycrystalline Pt surface in 0.5 M H_2SO_4 and in 1 M HCl, a broad band centered at 1100 cm^{-1} that increased in intensity as the potential was lowered from $+0.3$ to -0.06 V. The latter was found to disappear when the solvent was changed from H_2O to D_2O and thus, they proposed that the band be ascribed to either adsorbed H or H_3O^+. Thus, again we may say that these results are not inconsistent with the present study, although the presence

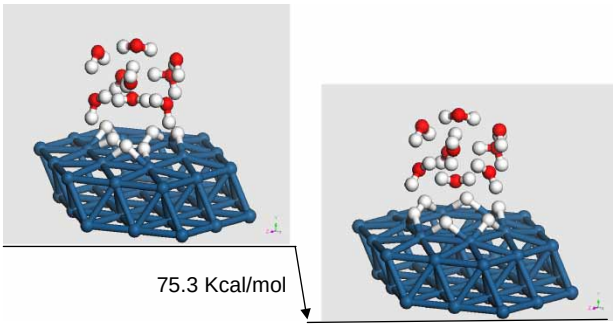

Figure 6. Diagram of relative energies of the $6H_{ads(bridge)}/Pt_{38}$/water system before and after self-assembly process at the potential of zero total charge ($\sim +0.2$ V versus RHE).

of all three crystal faces in the polycrystalline sample examined is a complicating factor.

As the number of H_{UPD} atoms increases, so does the exothermicity of the self-assembly process. Figure 6 displays a diagram of relative energies of the $6H_{UPD}/Pt_{38}$/water potential energy surface at $q = 0$ ($+0.2$ V versus RHE) before and after the self-assembly process of the six $H_{ads(bridge)}$. The spontaneous reorganisation of the six $H_{ads(bridge)}$ at this surface potential is exothermic by 75 kcal/mol, the energy released being more than *sevenfold* compared to that for three H_{UPD}. The unique self-assembly of the honeycomb structure spontaneously formed by the six H_{UPD} atoms is clearly demonstrated (Figure 6, right panel), with a coverage of 1.0 ML. The structures of H_{UPD} at two higher submonolayer coverages were also investigated, the first near the reversible potential and the second at the potential of zero total charge, by use of the DMOL-SOLID suite of programs of Accelrys Inc. [50]. Figure 7 displays the self-assembled hexagonal 2D honeycomb network of H_{UPD} for the first case. Surface-adsorbed hydrogen atoms begin to occupy on-top sites when all the hexagonal bridge sites are filled. Each $H_{ads(top)}$ tends to tilt slightly towards one of the six adjacent $H_{ads(bridge)}$ atoms, which in turn, tilts slightly away from the interacting $H_{ads(top)}$. At the more positive

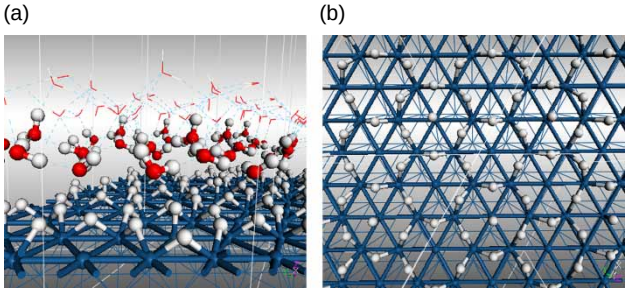

Figure 7. A self-assembled hexagonal 2D honeycomb network of H_{UPD} at high submonolayer coverage, near $+0.0$ V versus RHE. In the right panel (b), all the water molecules and the lower Pt layers are omitted for clarity.

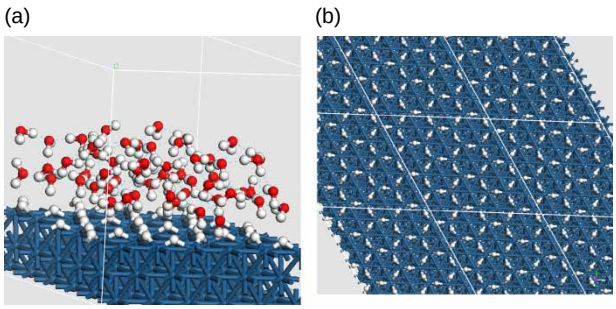

Figure 8. A self-assembled hexagonal 2D honeycomb network of H_{UPD} at a full coverage that approaches one H per surface Pt (i.e. 1 ML) at the potential of zero total charge. In the right panel (b), all the water molecules are omitted for clarity.

potential, we find that the on-top H atoms are completely absent (Figure 8). We note that the theoretically predicted coverage in Figure 8 (1 ML) is also not inconsistent with the experimentally observed maximum of $\sim$2/3 ML [16]; the coverage versus potential curve climbs linearly with increasingly negative potential, and thus the maximum coverage is not observable, due to the onset of the HER [57]. We note further that, at a potential intermediate between those of Figures 7 and 8, i.e. $\sim +0.1$ V versus RHE, the formation of on-top hydrogen is possible, according to our previous work and has been observed experimentally at such potentials [28,43]. These issues will be treated in more detail in a separate publication.

4. Summary

The first-principles direct MD simulation of HOR at submonolayer coverages of adsorbed $H_{ads(bridge)}$ shows that a heterolytic H—H bond cleavage takes place in the oxidative adsorption via the Heyrovsky process as the H_2 molecule approaches the surface at potentials more positive ($>+0.1$ V) than the reversible potential. The reaction products are the $H^+_{(aq)}$ and an additional inert $H_{ads(bridge)}$; as in our previous study, we identify the latter as H_{UPD}. The highly exothermic oxidation of molecular hydrogen imparts rapid site-to-site shifts of the newly created H_{UPD} along the metal surface, while the existing H_{UPD} atoms remain in bridge sites. The HOR does not induce oxidation of any of the submonolayer H_{UPD} atoms at potentials of $+0.2$ to $+0.3$ V versus RHE, since they lie nearly flat in their bridging positions on the metal surface and interact only very weakly with the aqueous phase of the metal/solution interface. Continued HOR leads to a higher submonolayer coverage of the Pt(111) surface by the adsorbed H_{UPD} atoms. The present quantum chemical simulation identifies a unique ordered signature reminiscent of other types of UPD states, in which the H_{UPD} atoms self-assemble to form a hexagonal 2D honeycomb network on the Pt(111) surface at submonolayer coverage. The potential dependence of the UPD H coverage is under investigation for the electrode

potentials more negative than the RHE to examine the role that H_{UPD} plays in HER [58].

Acknowledgements

The authors gratefully acknowledge financial support from the NASA-UPR Center for Nanoscale Materials under NASA URC Grant NCC3-1034. The authors gratefully acknowledge Drs R.R. Adzic, J.M. Feliu and K. Kunimatsu for helpful discussions.

References

[1] W. Vielstich, A. Lamm, and H.A. Gasteiger (eds), *Handbook of Fuel Cells*, Vol. 2, Wiley, New York, 2003.

[2] F.T. Wagner and P.N. Ross, *Long-range structural effects in the anomalous voltammetry on ultra-high vacuum prepared Pt(111)*, J. Electroanal. Chem. 250 (1988), pp. 301–320.

[3] A.V. Tripkovic and R.R. Adzic, *Hydrogen electrosorption of single-crystal platinum stepped surfaces and the effects of oxide formation*, J. Electroanal. Chem. 205 (1986), pp. 335–342.

[4] D. Armand and J. Clavilier, *Quantitative analysis of the distribution of the hydrogen adsorption states at platinum surfaces: Part I. Application to Pt(100) in sulphuric acid medium*, J. Electroanal. Chem. 225 (1987), pp. 205–214.

[5] K. Seto, A. Iannelli, B. Love, and J. Lipkowski, *The influence of surface crystallography on the rate of hydrogen evolution at Pt electrodes*, J. Electroanal. Chem. 226 (1987), pp. 351–360.

[6] R.J. Nichols and A. Bewick, *Spectroscopic identification of the adsorbed intermediate in hydrogen evolution on platinum*, J. Electroanal. Chem. 243 (1988), pp. 445–453.

[7] M. Wasberg, L. Palaikis, S. Wallen, M. Kamrath, and A. Wieckowski, *Leed/auger verification of the* in situ *method of preparation of Pt(111) single crystal electrodes*, J. Electroanal. Chem. 256 (1988), pp. 51–63.

[8] J. Clavilier, K.E. Actii, M. Petit, A. Rodes, and M.A. Zamakhchari, *Electrochemical monitoring of the thermal reordering of platinum single-crystal surfaces after metallographic polishing from the early stage to the equilibrium surfaces*, J. Electroanal. Chem. 295 (1990), pp. 333–356.

[9] N.S. Marinkovic, N.M. Markovic, and R.R. Adzic, *Hydrogen adsorption on single-crystal platinum electrodes in alkaline solutions*, J. Electroanal. Chem. 330 (1992), pp. 433–452.

[10] B.E. Conway and B.V. Tilak, *Interfacial processes involving electrocatalytic evolution and oxidation of H_2, and the role of chemisorbed H*, Electrochim. Acta 47 (2002), pp. 3571–3594.

[11] M. Baldauf and D.M. Kolb, *A hydrogen adsorption and absorption study with ultrathin Pd overlayers on Au(111) and Au(100)*, Electrochim. Acta 38 (1993), pp. 2145–2153.

[12] R. Gomez, A. Fernandez-Vega, J.M. Feliu, and A. Aldaz, *Hydrogen evolution on platinum single crystal surfaces: effects of irreversibly adsorbed bismuth and antimony on hydrogen adsorption and evolution on platinum (100)*, J. Phys. Chem. 97 (1993), pp. 4769–4776.

[13] J.M. Feliu, J.M. Orts, R. Gomez, A. Aldaz, and J. Clavilier, *New information on the unusual adsorption states of Pt(111) in sulphuric acid solutions from potentiostatic adsorbate replacement by CO*, J. Electroanal. Chem. 372 (1994), pp. 265–268.

[14] A. Peremans and A. Tadjeddine, *Electrochemical deposition of hydrogen on platinum single crystals studied by infrared-visible sum-frequency generation*, J. Chem. Phys. 103 (1995), pp. 7197–7203.

[15] J.J.T.T. Vermeijlen, L.J.J. Janssen, and G.J. Visser, *Mechanism of hydrogen oxidation on a platinum-loaded gas diffusion electrode*, J. Appl. Electrochem. 27 (1997), pp. 497–506.

[16] N.M. Markovic, B.N. Grgur, and P.N. Ross, *Temperature-dependent hydrogen electrochemistry on platinum low-index single-crystal surfaces in acid solutions*, J. Phys. Chem. B 101 (1997), pp. 5405–5413.

[17] A. Zolfaghari, M. Chayer, and G. Jerkiewicz, *Energetics of the underpotential deposition of hydrogen on platinum electrodes*, J. Electrochem. Soc. 144 (1997), pp. 3034–3041.

[18] J. Barber, S. Morin, and B.E. Conway, *Specificity of the kinetics of H_2 evolution to the structure of single-crystal Pt surfaces, and the relation between opd and upd H*, J. Electroanal. Chem. 446 (1998), pp. 125–138.

[19] N.M. Markovic, T.J. Schmidt, B.N. Grgur, H.A. Gasteiger, R.J. Behm, and P.N. Ross, *Effect of temperature on surface processes at the Pt(111)-liquid interface: Hydrogen adsorption, oxide formation, and CO oxidation*, J. Phys. Chem. B 103 (1999), pp. 8568–8577.

[20] M.R. Gennero de Chialvo and A.C. Chialvo, *The Tafel-Heyrovsky route in the kinetic mechanism of the hydrogen evolution reaction*, Electrochem. Commun. 1 (1999), pp. 379–382.

[21] B. Ren, X. Xu, X.Q. Li, W.B. Cai, and Z.Q. Tian, *Extending surface Raman spectroscopic studies to transition metals for practical applications: II. Hydrogen adsorption at platinum electrodes*, Surf. Sci. 427–428 (1999), pp. 157–161.

[22] E. Lamy-Pitara, S. El Mouahid, and J. Barbier, *Effect of anions on catalytic and electrocatalytic hydrogenations and on the electro-catalytic oxidation and evolution of hydrogen on platinum*, Electrochim. Acta 45 (2000), pp. 4299–4308.

[23] B.E. Conway and G. Jerkiewicz, *Relation of energies and coverages of underpotential and overpotential deposited H at Pt and other metals to the 'volcano curve' for cathodic H_2 evolution kinetics*, Electrochim. Acta 45 (2000), pp. 4075–4083.

[24] L. Giorgi, A. Pozio, C. Bracchini, R. Giorgi, and S. Turtú, *H_2 and H_2/CO oxidation mechanism on Pt/C, Ru/C and Pt–Ru/C electrocatalysts*, J. Appl. Electrochem. 31 (2001), pp. 325–334.

[25] M.C. Tavares, S.A.S. Machado, and L.H. Mazo, *Study of hydrogen evolution reaction in acid medium on Pt microelectrodes*, Electrochim. Acta 46 (2001), 4359.

[26] H. Kita, *Horiuti's generalized rate expression and hydrogen electrode reaction*, J. Mol. Catal. A: Chemical 199 (2003), pp. 161–174.

[27] J. Solla-Gullon, F.J. Vidal-Iglesias, P. Rodriguez, E. Herrero, J.M. Feliu, J. Clavilier, and A. Aldaz, In situ *surface characterization of preferentially oriented platinum nanoparticles by using electrochemical structure sensitive adsorption reactions*, J. Phys. Chem. B 108 (2004), pp. 13573–13575.

[28] K. Kunimatsu, H. Uchida, M. Osawa, and M. Watanabe, In situ *infrared spectroscopic and electrochemical study of hydrogen electro-oxidation on Pt electrode in sulfuric acid*, J. Electroanal. Chem. 587 (2006), pp. 299–307.

[29] J.X. Wang, T.E. Springer, and R.R. Adzic, *Dual-pathway kinetic equation for the hydrogen oxidation reaction on Pt electrodes*, J. Electrochem. Soc. 153 (2006), pp. A1732–A1740.

[30] A.B. Anderson and Y. Cai, *Calculation of the Tafel Plot for H_2 oxidation on Pt(100) from potential-dependent activation energies*, J. Phys. Chem. B 108 (2004), pp. 19917–19920.

[31] A.B. Anderson, R.A. Sidik, J. Narayanasamy, and P. Shiller, *Theoretical calculation of activation energies for $Pt + H^+(aq) + e^- <=> Pt\text{-}H$: activation energy-based symmetry factors in the Marcus normal and inverted regions*, J. Phys. Chem. B 107 (2003), pp. 4618–4623.

[32] A.B. Anderson and T.V. Albu, Ab initio *determination of reversible potentials and activation energies for outer-sphere oxygen reduction to water and the reverse oxidation reaction*, J. Amer. Chem. Soc. 121 (1999), pp. 11855–11863.

[33] M. Aryanpour, V. Rai, and H. Pitsch, *Convergent iterative constrained variation algorithm for calculation of electron-transfer transition states*, J. Electrochem. Soc. 153 (2006), pp. E52–E57.

[34] J.-S. Filhol and M. Neurock, *Elucidation of the electrochemical activation of water over Pd by first principles*, Angew. Chem. Int. Ed. 45 (2006), pp. 402–406.

[35] A. Perez, M.J. Vilkas, C.R. Cabrera, and Y. Ishikawa, *Density functional theory study of water activation and COads + OHads reaction on pure platinum and bimetallic platinum/ruthenium nanoclusters*, J. Phys. Chem. B 109 (2005), pp. 23571–23578.

[36] M.T.M. Koper and G.A. Voth, *A three-dimensional potential energy surface for dissociative adsorption and associative desorption at metal electrodes*, J. Chem. Phys. 109 (1998), pp. 1991–2001.
[37] D. Dominguez-Ariza, C. Hartnig, C. Sousa, and F. Illas, *Combining molecular dynamics and* ab initio *quantum-chemistry to describe electron transfer reactions in electrochemical environments*, J. Chem. Phys. 121 (2004), pp. 1066–1073.
[38] C. Hartnig and M.T.M. Koper, *Solvent reorganization in electron and ion transfer reactions near a smooth electrified surface: a molecular dynamics study*, J. Am. Chem. Soc. 125 (2003), pp. 9840–9845.
[39] Y. Wang and P.B. Balbuena, *Roles of proton and electric field in the electroreduction of O_2 on Pt(111) surfaces: results of an* ab initio *MD study*, J. Phys. Chem. B 108 (2004), pp. 4376–4384.
[40] C. Hartnig and E. Spohr, *The role of water in the initial steps of methanol oxidation on Pt(111)*, Chem. Phys. 319 (2005), pp. 185–191.
[41] S.K. Desai and M. Neurock, *First-principles study of the role of solvent in the dissociation of water over a Pt-Ru alloy*, Phys. Rev. B 68 (2003), 075420.
[42] J.X. Wang, T.E. Springer, P. Liu, M. Shao, and R.R. Adzic, *Hydrogen oxidation reaction on Pt in acidic media: adsorption isotherm and activation free energies*, J. Phys. Chem. C 111 (2007), pp. 12425–12433.
[43] K. Kunimatsu, T. Senzaki, G. Samjeske, M. Tsushima, and M. Osawa, *Hydrogen adsorption and hydrogen evolution reaction on a polycrystalline Pt electrode studied by surface-enhanced infrared absorption spectroscopy*, Electrochim. Acta 52 (2007), pp. 5715–5724.
[44] Y. Ishikawa, J.J. Mateo, D.A. Tryk, and C.R. Cabrera, *Direct molecular dynamics and density-functional theoretical study of the electrochemical hydrogen oxidation reaction and underpotential deposition of H on Pt(111)*, J. Electroanal. Chem. 607 (2007), pp. 37–46.
[45] T. Ikegami, N. Kurita, H. Sekino, and Y. Ishikawa, *Mechanism of cis-to-trans isomerization of azobenzene: direct MD study*, J. Phys. Chem. A 107 (2003), pp. 4555–4562.
[46] H. Sellers, E.M. Pattrito, and P. Paredes-Olivera, *Adsorption of sulfate, bisulfate and sulfuric acid on silver surfaces: a theoretical study*, Surf. Sci. 418 (1998), pp. 376–394.
[47] B.E. Spiewak, R.D. Cortright, and J.A. Dumesic, *Microcalorimetric studies of H_2, C_2H_4, and C_2H_2 adsorption on Pt powder*, J. Catal. 176 (1998), pp. 405–414.
[48] G.W. Watson, R.P.K. Wells, D.J. Willock, and G.J. Hutchings, *A comparison of the adsorption and diffusion of hydrogen on the {111} surfaces of Ni, Pd, and Pt from density functional theory calculations*, J. Phys. Chem. B 105 (2001), pp. 4889–4894.
[49] J. Greeley and M. Mavrikakis, *Surface and subsurface hydrogen: adsorption properties on transition metals and near-surface alloys*, J. Phys. Chem. B 109 (2005), pp. 3460–3471.
[50] (a) B. Delley, *An all-electron numerical method for solving the local density functional for polyatomic molecules*, J. Chem. Phys. 92 (1990), pp. 508–517; (b) B. Delley, *From molecules to solids with the DMol^3 approach*, J. Chem. Phys. 113 (2000), pp. 7756–7764.
[51] J.P. Perdew, K. Burke, and M. Ernzerhof, *Generalized gradient approximation made simple*, Phys. Rev. Lett. 77 (1996), pp. 3865–3868.
[52] D. Marx, M.E. Tuckerman, J. Hutter, and M. Parrinello, *The nature of the hydrated excess proton in water*, Nature 397 (1999), pp. 601–604.
[53] K. Christmann, *Interaction of hydrogen with solid surfaces*, Surf. Sci. Rep. 9 (1988), pp. 1–163.
[54] E. Skúlason, G.S. Karlberg, J. Rossmeisl, T. Bligaard, J. Greeley, H. Jónsson, and J.K. Nørskov, *Density functional theory calculations for the hydrogen evolution reaction in an electrochemical double layer on the Pt(111) electrode*, Phys. Chem. Chem. Phys. 9 (2007), pp. 3241–3250.
[55] J.J. Mateo and Y. Ishikawa, to be published.
[56] W. Ho, R.F. Willis, and E.W. Plummer, *Observation of nondipole electron impact vibrational excitations: H on W (100)*, Phys. Rev. Lett. 40 (1978), pp. 1463–1466.
[57] A. Lasia, *Modeling of hydrogen upd isotherms*, J. Electroanal. Chem. 562 (2004), pp. 23–31.
[58] M. Otani, I. Hamada, O. Sugino, Y. Morikawa, Y. Okamoto, and T. Ikeshoji, *Electrode dynamics from first principles*, J. Phys. Soc. Jpn. 77 (2008), 024802.